Available online at www.sciencedirect.com
SCIENCE DIRECT
Journal of Power Sources 154 (2006) 239–245
JOURNAL OF POWER SOURCES
www.elsevier.com/locate/jpowsour

Synthesis and electrochemical properties of $LiAl_{0.1}Mn_{1.9}O_4$ by microwave-assisted sol–gel method

Shu-Juan Bao, Yan-Yu Liang, Wen-Jia Zhou, Ben-Lin He, Hu-Lin Li *

College of Chemistry and Chemical Engineering of Lanzhou University, Lanzhou 730000, PR China

Received 19 November 2004; received in revised form 11 March 2005; accepted 25 March 2005
Available online 6 June 2005

Abstract

Aluminum-doped spinel-type $LiMn_2O_4$ cathode active materials have been synthesized by a microwave-assisted sol–gel method. The influence of synthesis conditions on the structural and electrochemical properties of $LiAl_{0.1}Mn_{1.9}O_4$ was investigated by thermo-gravimetric analysis (TGA), X-ray diffraction (XRD), scanning electron microscopy (SEM), and charge/discharge experiments. The powders resulting from the microwave-assisted sol–gel method with good crystallinity and cubic spinel shapes deliver an initial discharge capacity of 120 mAh g^{-1}, present excellent rate capability, and the Coulombic efficiency of it almost approaches 99% after 30 cycles. These advantages make it attractive particularly for a practical application. In addition, cyclic voltammetry (CV) and electrochemical impedance spectroscopy (EIS) were employed to characterize the reactions of Li ion insertion into and extraction from $LiAl_{0.1}Mn_{1.9}O_4$ electrodes.

Keywords: Lithium-ion batteries; Spinel-type; $LiAl_{0.1}Mn_{1.9}O_4$; Microwave

1. Introduction

Rechargeable lithium-ion batteries have become a commercial reality in recent years. They are incorporated in a multitude of mobile electronic equipments. The global projections for the marketing of portable electronic devices with extraordinary capabilities create a very strong driving force for R&D of light, efficient, environmentally friendly, and cheap rechargeable lithium-ion batteries [1,2].

Currently, the choice for the cathode material is $LiCoO_2$, which although has good capacity and recharge-ability, suffers from the high cost and environmental toxicity of cobalt [3]. Consequently, much effort has been put into developing alternatives. At present, the materials most likely to succeed in future commercial applications are $LiMn_2O_4$ and related derivatives due to the low cost and nontoxicity of manganese, so an intensive research of that has been underway in recent years [4,5].

Although $LiMn_2O_4$ has some merits, it still has difficulty for practical application, owing to severe capacity fading. The reason why spinel $LiMn_2O_4$ shows capacity loss during cycling is not identified clearly yet, and several possible sources are suggested [4–7], such as Jahn–Teller distortion, lattice instability, manganese dissolution, electrolyte decomposition, and so on. To overcome capacity fading, the manganese site was replaced by some of transition metals, such as Co [8], Ni [8,9], Fe [8,10], Cr [10,11], Zn [12], Cu [13], etc., to enhance structural stability. Since the aluminum is abundant, less expensive, and lighter than the transition metal group, Al-substituted $LiMn_2O_4$ is expected to be a cathode material with lower cost than transition metals substituted $LiMn_2O_4$. Furthermore, many researchers [14–16] have reported the lithium intercalation properties of $LiAl_xMn_{2-x}O_4$. It suggests that Al-doped $LiMn_2O_4$ showed relatively good cycling performances.

There are other factors that influence the quality of $LiMn_2O_4$ powders used for lithium secondary batteries, such as particle size and surface morphology [3]. However, it is difficult to control such factors using a conventional solid-state reaction, which consists of extensive mechanical mixing and

* Corresponding author. Tel.: +86 931 891 2517; fax: +86 931 891 2582.
E-mail address: lihl@lzu.edu.cn (H.-L. Li).

0378-7753/$ – see front matter © 2005 Elsevier B.V. All rights reserved.
doi:10.1016/j.jpowsour.2005.03.220

extended grinding process that are detrimental to the quality of the final product. In order to solve this problem, a sol–gel method has been introduced [17,18]. Yet, it does not appear to be greatly advantageous over the solid-state reaction in terms of long reaction time. Recently, a novel method, known as the microwave synthesis method, was developed to prepare cathode materials for lithium-ion battery [19–21]. In the microwave irradiation field, since the microwave energy is absorbed directly by the bulk of the heated object, uniform and rapid heating can be achieved within several minutes. Therefore, the reaction time can be significantly decreased. With these considerations, an improved sol–gel method, that is microwave-assisted sol–gel method, has been used to synthesize positive electrode materials in this work.

In this study, an attempt was made to stabilize the spinel structure by improving the synthesis method. The $LiMn_2O_4$ partly substituted the manganese site with one of the typical elements, aluminum, was successfully prepared by microwave-assisted sol–gel method. The physical characteristics and electrochemical properties of the synthesized products were investigated in detail. The results have indicated that the obtained $LiAl_{0.1}Mn_{1.9}O_4$ shows good performance as the lithium-ion batteries cathode material.

2. Experimental

2.1. Materials preparation

All the chemical reagents used in the experiments were analytical grade without further purification. $LiAl_{0.1}Mn_{1.9}O_4$ powders were synthesized by microwave-assisted sol–gel method using citric acid as a chelating agent. A stoichiometric amount of lithium acetate [$Li(CH_3COO)\cdot 2H_2O$], manganese acetate [$Mn(CH_3COO)_2\cdot 4H_2O$], and aluminum nitrate [$Al(NO_3)\cdot 9H_2O$] were dissolved in distilled water and mixed with aqueous solution of citric acid. The resulting solution was mixed with continuous magnetic stirring at 90 °C until a clear viscous gel occurs. The obtained precursor was preserved under vacuum at 100 °C for 12 h to eliminate water adequately and then was placed in microwave oven. The microwave power operated at 100% (650 W) for 20 min. After the microwave treatment, the samples were sintered at 750 °C for 10 h, followed by cooling to room temperature slowly. In addition, $LiAl_{0.1}Mn_{1.9}O_4$ was also prepared following the same procedure without microwave treatment for comparison (that is, traditional sol–gel method).

2.2. Structure and morphology characterization

Thermo-gravimetric analysis (TGA) was performed on Setarm TGDTA92A with α-Al_2O_3 as the reference substance at a heating rate of 10 °C min^{-1}. The structure of products was characterized by X-ray diffraction (XRD). XRD datum were collected by MAC M18XCE diffractometer with Cu Kα radiation (λ = 1.54056 Å) operating at 50.0 kV and 200.0 mA. SEM (JSM-5600LV, Japan) was used to observe the morphology of the products.

2.3. Electrochemical measurements

Powders of the as-prepared cathode materials were mixed with 15 wt% acetylene black. Five weight percent of polyvinylidene fluoride (PVDF) binder dissolved in *N*-methyl pyrrolidone (NMP) was added until a slurry was obtained. The slurry was pasted on aluminum foil followed by drying under vacuum at 100 °C for 24 h. The cell consisted of the cathode, Li metal as the anode, and an electrolyte of 1 M $LiPF_6$ in a 1:1 (v/v) mixture of ethylene carbonate (EC) and dimethyl carbonate (DMC). Celgard 2400 membrane was used as the cell separator. The assembly of the cells was conducted in an Ar-filled glove box. The cells were charged and discharged from 3.0 to 4.4 V at a current rate of *C*/3, except where otherwise specified, on Land CT2001A (China). Cyclic voltammetry measurements of the prepared powders were performed in the voltage range 3.0–4.5 V at a scan rate of 0.1 mV s^{-1}. The electrochemical impedance measurements were carried out by applying 100 kHz to 0.01 Hz frequency ranges with acoscillation amplitude of 5 mV. Both of the latest two electrochemical measurements were done using a CHI760 model Electrochemical Workstation (CH Instruments).

3. Results and discussion

3.1. TGA and XRD studies

The thermal properties of the obtained $LiAl_{0.1}Mn_{1.9}O_4$ precursor and the sample prepared by microwave-treated 20 min were studied using TG analysis. Fig. 1a displays the TG curve for the $LiAl_{0.1}Mn_{1.9}O_4$ precursor. It shows a first

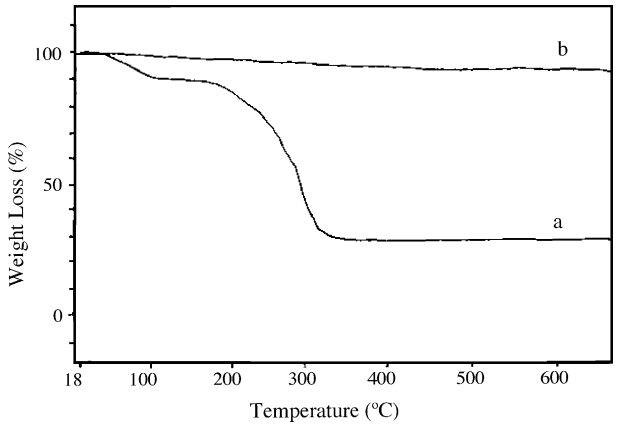

Fig. 1. The thermo-gravimetric analysis curves for (a) the $LiAl_{0.1}Mn_{1.9}O_4$ precursor and (b) the $LiAl_{0.1}Mn_{1.9}O_4$ obtained by microwave-treated 20 min.

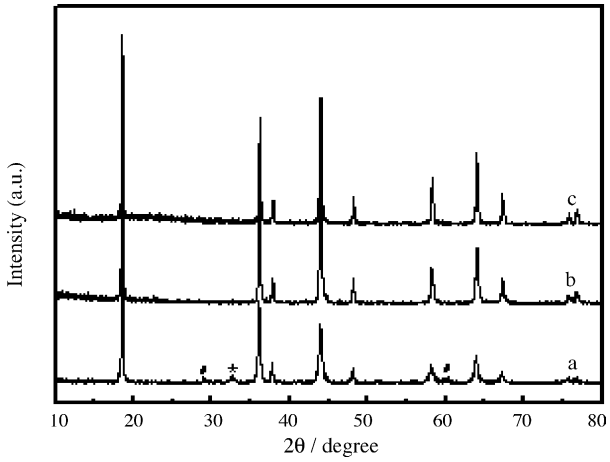

Fig. 2. The XRD patterns of $LiAl_{0.1}Mn_{1.9}O_4$ obtained by different heat-treated methods and processes. (a) The $LiAl_{0.1}Mn_{1.9}O_4$ obtained by microwave-treated 20 min, (b) the $LiAl_{0.1}Mn_{1.9}O_4$ obtained by microwave-assisted sol–gel method, and (c) the $LiAl_{0.1}Mn_{1.9}O_4$ prepared by traditional sol–gel method (key: (+) Mn_2O_3, (#) unidentified phase).

weight loss of ~9.5% around 141 °C, which is attributed to the evaporation of residual water. The second weight loss of ~9.6% is around 213 °C, which is due to the removal of chemically bound water in the sample. The third step weight loss of 49.9% around 300 °C corresponds to the decomposition of organics and the formation of $LiAl_{0.1}Mn_{1.9}O_4$ phase. The weight loss between 400 and 700 °C is very little. This behavior implies that the formation of $LiAl_{0.1}Mn_{1.9}O_4$ phase is completed at this stage. Fig. 1b shows the TG curve for the $LiAl_{0.1}Mn_{1.9}O_4$ obtained by microwave-treated 20 min, which indicates that the weight loss is very little during the whole heating process. It is ascribed to most of the $LiAl_{0.1}Mn_{1.9}O_4$ spinel phase has been formed during the microwave-treated process.

Fig. 2 illustrates the XRD patterns of the $LiAl_{0.1}Mn_{1.9}O_4$ synthesized by different methods. The powder obtained by microwave-treated 20 min has transformed into cubic spinel structure (this is in agreement with the TG analysis above), however, the impurity peaks of Mn_2O_3 (marked by +) and other unidentified phase (marked by #) also retained in the spinel LMO phase. Probably, large amount of carbon contents in the precursor (lithium acetate, manganese acetate, and citric acid) tend to reduce manganese ions during microwave-treated process and favors the formation of Mn_2O_3 impurities [22,23]. After further sintering for 10 h, the impurity Mn_2O_3 phase completely disappeared and the powder crystallized into pure cubic spinel structure as indicated by Fig. 2b. Fig. 2c displays the XRD patterns of the $LiAl_{0.1}Mn_{1.9}O_4$ obtained by traditional sol–gel method. Evidently, it exhibits striking similarity to those of the $LiAl_{0.1}Mn_{1.9}O_4$ prepared by microwave-assisted sol–gel method. All of the diffraction peaks were assigned to the spinel compound. The result is in good accordance with the standard spectrum (JCPDS, Card No. 35-0782).

The lattice constant of $LiAl_{0.1}Mn_{1.9}O_4$ obtained by microwave-assisted sol–gel method, which is on the basis of a least square refinement program, is calculated to be 8.216 Å. The value is a little smaller than 8.247 Å of the standard spinel $LiMn_2O_4$.

Several researchers have also demonstrated that the aluminum-doped compounds have cubic spinel structure. Due to the smaller ionic radii of aluminum ions (Al^{3+}, 0.53 Å) than manganese ions (Mn^{3+}, 0.66 Å; Mn^{4+}, 0.60 Å) [24], the substitution manganese with aluminum results in shrinkage of the unit cell volume. In addition, the bonding energy of Al–O (512 kJ mol^{-1}) is stronger than that of the Mn–O (402 kJ mol^{-1}) bond, which enhances the stability of the spinel structure during insertion and deinsertion of lithium [3,24], and decreases the capacity loss of the $Li/LiAl_{0.1}Mn_{1.9}O_4$ cells after many cycles.

3.2. SEM studies

Fig. 3 shows the scanning electron microscope (SEM) images for the $LiAl_{0.1}Mn_{1.9}O_4$ synthesized by traditional sol–gel and microwave-assisted sol–gel method. Comparing Fig. 3a with b, there is a significant difference between the

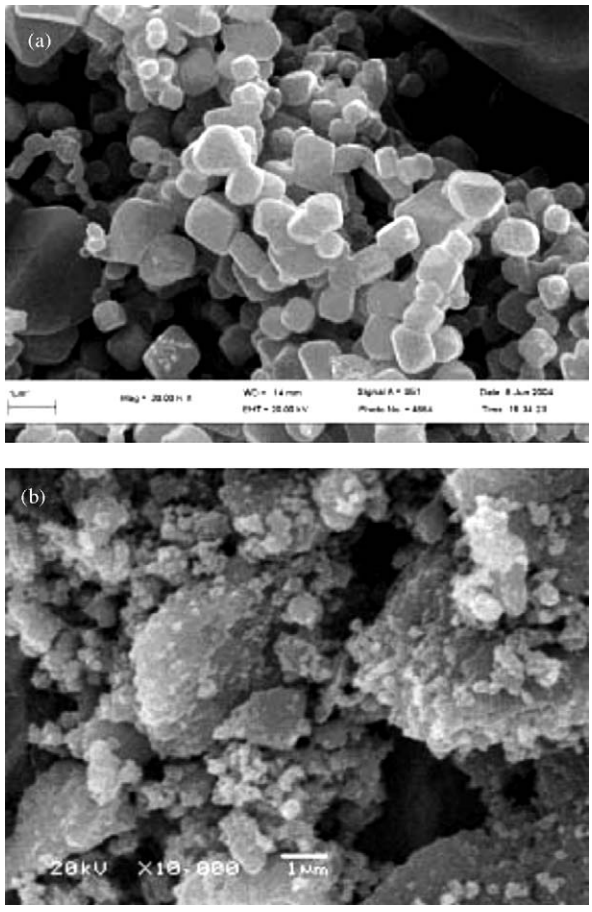

Fig. 3. SEM images of the $LiAl_{0.1}Mn_{1.9}O_4$ obtained by microwave-assisted sol–gel method (a) and the $LiAl_{0.1}Mn_{1.9}O_4$ obtained by traditional sol–gel method (b).

two samples. The particles of $LiAl_{0.1}Mn_{1.9}O_4$ obtained by microwave-assisted sol–gel method are distributed uniformly and have good cubic structure shapes. The well-dispersed particles are the result of the treatment of microwave as reported by literature [25], because the microwave heated not from the outside but from the inside of the precursor and thus provided a uniform heating environment which shortened the synthesizing time and overcame the agglomeration of particles. Such kind of morphology is very important to both the high specific capacity and good cyclability of the materials [25,26].

3.3. Electrochemical properties

In order to study the influence of different synthesis methods on the cycle behavior, the cells were tested at a charge/discharge current rate of *C*/3 between 3.0 and 4.4 V. The variations of the discharge capacity with the cycle number for $LiAl_{0.1}Mn_{1.9}O_4$ powders prepared under different synthesis conditions are shown in Fig. 4. For the sample obtained by microwave-treated 20 min, the discharge capacity is relatively low and fades very fast. However, when it was calcined at 750 °C for 10 h, the discharge capacity increased significantly and the cycling behavior of the powders became much better. This is probably explained as that the microwave treatment, which delivers an impure Li–Mn–O spinel with Mn_2O_3 phase (this can be confirmed by XRD analysis), during cycling, the unit cell of the incomplete growth $LiAl_{0.1}Mn_{1.9}O_4$ crystallites will distort, so its capacity decreased rapidly. After following sintering for 10 h, the $LiAl_{0.1}Mn_{1.9}O_4$ has a very well order Li–Mn–O spinel without any other impure phases, hence, its capacity increase significantly. Comparing Fig. 4a with b, the $LiAl_{0.1}Mn_{1.9}O_4$ prepared by microwave-assisted sol–gel method presented

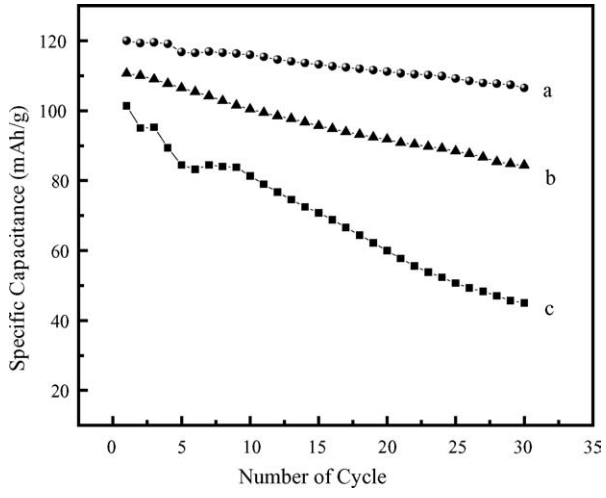

Fig. 4. The typical discharge capacity versus the cycle number for the $LiAl_{0.1}Mn_{1.9}O_4$ obtained by different synthesis conditions. (a) $LiAl_{0.1}Mn_{1.9}O_4$ obtained by microwave-assisted sol–gel method, (b) the $LiAl_{0.1}Mn_{1.9}O_4$ prepared by traditional sol–gel method, and (c) $LiAl_{0.1}Mn_{1.9}O_4$ obtained by microwave-treated 20 min.

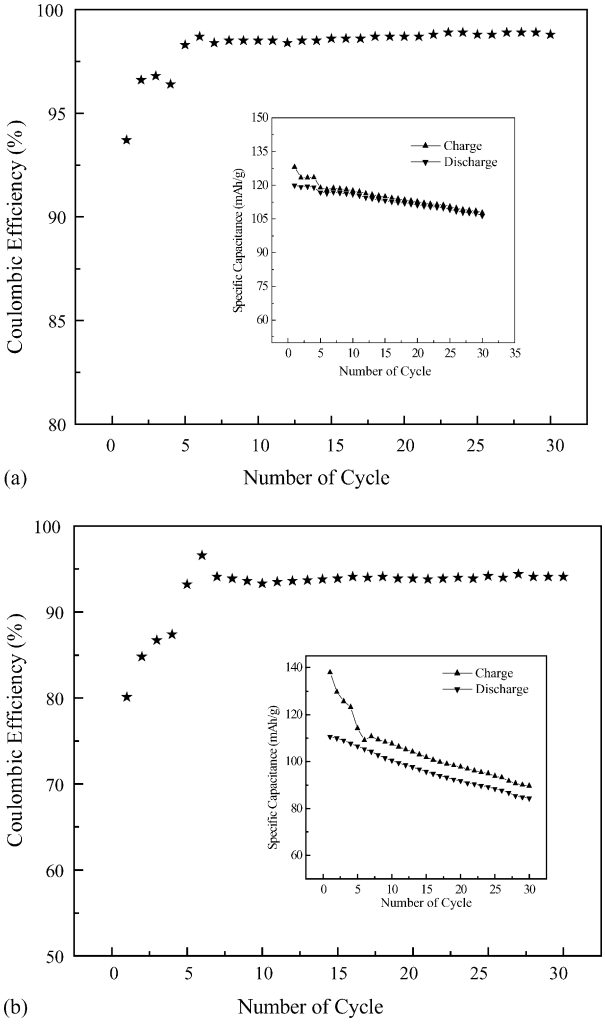

Fig. 5. The Coulombic efficiency for charge/discharge as a function of cycle number for the $LiAl_{0.1}Mn_{1.9}O_4$ obtained by different methods. (a) The $LiAl_{0.1}Mn_{1.9}O_4$ obtained by microwave-assisted sol–gel method and (b) the $LiAl_{0.1}Mn_{1.9}O_4$ prepared by traditional sol–gel method.

a higher discharge capacity and better capacity retention than that of the $LiAl_{0.1}Mn_{1.9}O_4$ obtained by traditional sol–gel method. The result indicates the samples obtained by microwave-assisted sol–gel have a better crystallinity (due to the limit resolution of XRD method, this cannot be seen from XRD) and regular morphology.

The Coulombic efficiency for charge/discharge as a function of cycle number is shown in Fig. 5. It can be found that the Coulombic efficiency increases with growth of cycle numbers for the two samples, which indicates that the reversibility of charge/discharge increases. At the 30 cycles, the Coulombic efficiency almost approaches 99% for the $LiAl_{0.1}Mn_{1.9}O_4$ prepared by microwave-assisted sol–gel method and 94% for the sample obtained by traditional sol–gel method, respectively. It is well known that Coulombic efficiency is an important index in assessing the quality of lithium-ion battery. Therefore, the results obtained above further confirm that microwave-assisted sol–gel method appears to be a bet-

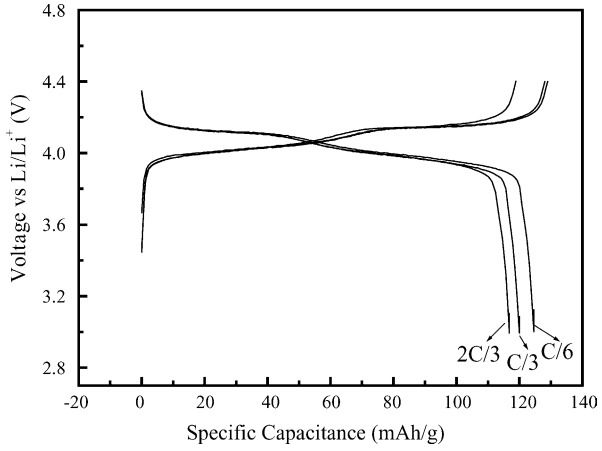

Fig. 6. The charge/discharge curves of the $LiAl_{0.1}Mn_{1.9}O_4$ obtained by microwave-assisted sol–gel method at *C*/6, *C*/3, and 2*C*/3.

ter alternative to the traditional sol–gel method for preparing lithium-ion battery cathode materials. Hence, further tests were focused on the $LiAl_{0.1}Mn_{1.9}O_4$ prepared by microwave-assisted sol–gel method in this study.

Fig. 6 displays the voltage versus specific discharge capacity profiles of the Li/$LiAl_{0.1}Mn_{1.9}O_4$ cell discharged at different current rates (*C*/6, *C*/3, and 2*C*/3). It exhibits remarkable rate capability. The 2*C*/3 discharge capacity is 93% of that discharged at *C*/6. Because a high rate discharge capability is one of the most important electrochemical performances in the application of electrode and battery [27], the excellent rate capability of the sample makes it attractive particularly for a practical application.

The cyclic voltammogram of the sample is displayed in Fig. 7. The anodic and cathodic peaks observed in the CV of the $LiAl_{0.1}Mn_{1.9}O_4$ powder exhibits reversible oxidation and reduction reactions corresponding to Li extraction and insertion. The split of the redox peaks into two couples indicates that the electrochemical reactions of the insertion and extraction of Li ion proceed in two stages [18,28]. In the

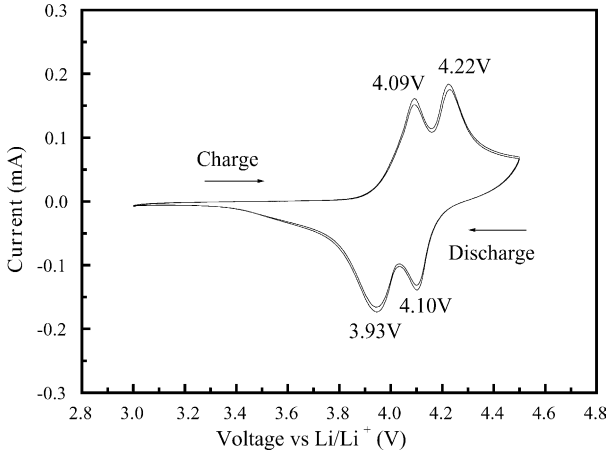

Fig. 7. The cyclic voltammogram of $LiAl_{0.1}Mn_{1.9}O_4$ obtained by microwave-assisted sol–gel method at a 0.1 mV s^{-1} scan rate.

spinel $LiAl_{0.1}Mn_{1.9}O_4$, Li ions occupy tetrahedral sites (8a), Mn^{3+}, Mn^{4+} ions and little amount of Al^{3+} reside at the octahedral sites (16d), and O^{2-} ions locate at 32e sites [29]. The oxygen ions form a cubic close-packed array, tetrahedral sites (8a) share face with vacant octahedral sites (16c), and so that they form a three-dimensional vacant channels.

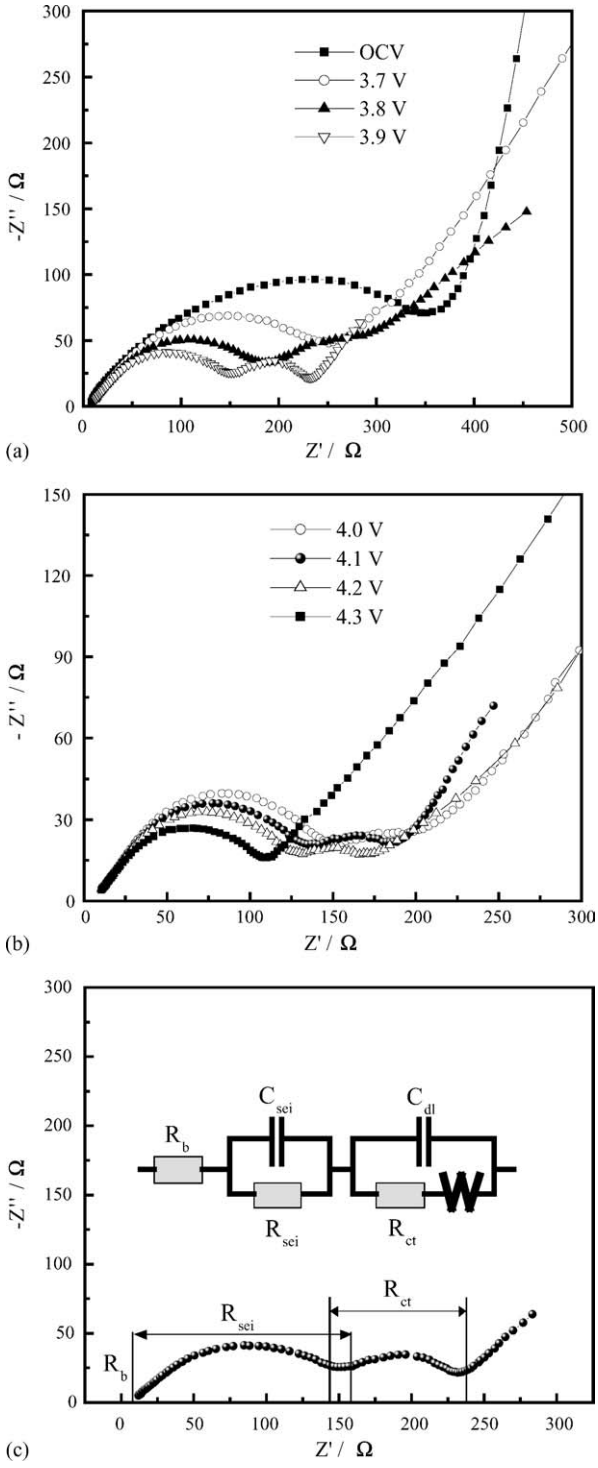

Fig. 8. Typical EIS of the Li/$LiAl_{0.1}Mn_{1.9}O_4$ cell and the equivalent circuit used to fit the EIS.

Li ions can intercalate/deintercalate through these channels during the electrochemical reaction [23]. The first oxidation peak at approximately 4.09 V is attributed to the removal of Li ions from half of the tetrahedral sites, whereas the second oxidation peak at approximately 4.22 V is thought to be due to the removal of Li ions from the remaining tetrahedral sites.

A typical EIS of the Li/$LiAl_{0.1}Mn_{1.9}O_4$ half-cell is shown in Fig. 8. As could be seen from the plots, in most of voltage range, the EIS of the Li/$LiAl_{0.1}Mn_{1.9}O_4$ half-cell is composed of two partially overlapped semicircles and a straight slopping line. Such a pattern of the EIS can be fitted by an equivalent circuit shown in inset of Fig. 8c. The R_b is bulk resistance of the cell, which reflects electric conductivity of the electrolyte, separator, and electrodes; R_{sei} and C_{sei} are the resistance and the capacitance of the solid-state interface layer formed on the surface of the electrodes, which correspond to the semicircle at high frequencies; R_{ct} and C_{dl} are the Faradic charge-transfer resistance and its relative double layer capacitance, corresponding to the semicircle at medium frequencies; W is the Warburg impendence related to a combination of the diffusional effects of Li ion on the interface between the active material particles and electrolyte, which is generally indicated by a straight sloping line at low frequency end. The combination of R_{ct} and W is called Faradic impedance, which reflects kinetics of the cell reactions. Total resistance (R_{cell}) of the Li/$LiAl_{0.1}Mn_{1.9}O_4$ cell is shown in Fig. 8c, which is mainly contributed to the R_b, R_{sei}, and R_{ct}, but not a simply summation of those three individual values.

It can be seen from Fig. 8a and b, in the voltage range from open circuit voltage (OCV) to 4.3 V, the R_b remains unchanged while the R_{sei} and R_{ct} vary significantly. The R_{sei} of the Li/$LiAl_{0.1}Mn_{1.9}O_4$ cell evidently decreases when Li ions deintercalated from the cathode in the voltage range from OCV to 4.3 V. This can be speculated that such a change in the R_{sei} origins from a reconstruction of the solid-state interface layer on the electrode surface caused by contraction and expansion of the electrode volume during the processes of deintercalation and intercalation of Li ions [29]. Over the whole voltage range, the change of R_{ct} is much larger than that of either the R_b or R_{sei}. The second semicircles are not observed when the working electrodes are at OCV state and 4.3 V. This is due to R_{ct} closely associated with the kinetics of the cell reaction.

4. Conclusions

This work demonstrated that the spinel-phased, well-crystallized $LiAl_{0.1}Mn_{1.9}O_4$ powders could be effectively synthesized via the microwave-assisted sol–gel process. In comparison with the conventional sol–gel method, microwave-assisted sol–gel process is superior in terms of shorter reaction time and regular cubic spinel shapes. TGA and XRD studies of the material obtained by microwave-treated 20 min have confirmed that spinel phase formed during microwave-treated process. Electrochemical test of the as-prepared samples as cathode for Li ion batteries has shown that further sintering improved significantly the quality of $LiAl_{0.1}Mn_{1.9}O_4$, which displays excellent rate capability, high Coulombic efficiency, and good reversibility. All of these above-mentioned make it attractive particularly for a practical application. Future research to optimize the composition and sintering time, particularly to further increase the cyclability is currently in progress.

Acknowledgement

The authors are thankful for the support provided by National Nature Science Foundation of China (No. 60471014).

References

[1] J.M. Tarascon, M. Armand, Nature 414 (2001) 359.
[2] V. Ganesh Kumar, J.S. Ganaraj, S. Ben-David, D.M. Pickup, R.H. Ernst, A. Van-Eck, D. Gedanken, Aurbach Chem. Mater. 15 (2003) 4211.
[3] Y.K. Sun, C.S. Yoon, C.K. Kim, S.G. Youn, Y.S. Lee, M. Yoshio, I.H. Oh, J. Mater. Chem. 11 (2001) 2519.
[4] D.H. Jang, Y.J. Shin, S.M. Oh, J. Electrochem. Soc. 143 (1996) 2204.
[5] Y. Xia, Y. Zhou, M. Yoshio, J. Electrochem. Soc. 144 (1997) 2593.
[6] P. Arora, B.N. Popov, R.E. White, J Electrochem. Soc. 145 (1998) 807.
[7] S.T. Myung, H.T. Chung, S. Komaba, N. Kumagai, H.B. Gu, J. Power Sources 90 (2000) 103.
[8] H.J. Bang, V.S. Donepudi, J. Prakash, Electrochim. Acta 48 (2002) 443.
[9] K. Amine, H. Tukamoto, H. Yasuda, Y. Fujita, J. Electrochem. Soc. 143 (1996) 1607.
[10] Y.P. Fu, Y.H. Su, C.H. Lin, Solid State Ionics 166 (2004) 137.
[11] C.H. Lu, Y. Lin, H.C. Wang, J. Mater. Sci. Lett. 22 (2003) 615.
[12] Q. Feng, H. Kanoh, Y. Miyai, K. Doi, Chem. Mater. 7 (1995) 379.
[13] R. Thirunakaran, B.R. Babu, N. Kalaiselvi, P. Periasamy, T.P. Kumar, N.G. Renganathan, M. Ragharan, N. Muniyandi, Bull. Mater. Sci. 24 (2001) 51.
[14] A. Amatucci, A. Du Pasquier, A. Blyr, T. Zheng, J.M. Tarascon, Electrochim. Acta 45 (1999) 255.
[15] S.H. Park, K.S. Park, Y.K. Sun, K.S. Nahm, J. Electrochem. Soc. 147 (2000) 2116.
[16] S.T. Myung, S. Komaba, N. Kumagai, J. Electrochem. Soc. 148 (2001) 482.
[17] J.H. Choy, D.H. Kim, C.W. Kwon, S.J. Hwang, Y.I. Kim, J. Power Sources 77 (1999) 1.
[18] X.M. Wu, X.H. Li, Z.B. Xiao, J.B. Liu, W.B. Yan, M.Y. Ma, Mater. Chem. Phys. 84 (2004) 182.
[19] P.S. Whitfield, I.J. Davidson, J. Electrochem. Soc. 147 (2000) 4476.
[20] H. Yan, X. Huang, H. Li, L. Chen, J. Power Sources 81–82 (1999) 647.
[21] H. Yan, X. Huang, H. Li, L. Chen, Solid State Ionics 11 (1998) 113.
[22] S. Choi, A. Manthiram, J. Electrochem. Soc. 147 (2000) 1623.
[23] N. Santander, S.R. Das, S.B. Majumder, R.S. Katiyar, Surf. Coat. Technol. 177–178 (2004) 60.

[24] G.G. Amatucci, N. Pereira, T. Zheng, I. Plitz, J.M. Tarascon, J. Power Sources 81–82 (1999) 39.
[25] S.T. Yang, Y.F. Zhang, Q.Z. Lv, J. Inorg. Mater. 15 (2000) 312.
[26] F.K. Shokoohi, J.M. Tarascon, B.J. Wilkens, D. Guyomard, C.C. Chang, J. Electrochem. Soc. 139 (1992) 1847.
[27] S.H. Ye, J.Y. Lv, X.P. Gao, F. Wu, D.Y. Song, Electrochim. Acta 49 (2004) 1623.
[28] Y. Xia, M. Yoshio, J. Electrochem. Soc. 143 (1996) 825.
[29] S.S. Zhang, K. Xu, T.R. Jow, Electrochim. Acta 49 (2004) 1057.